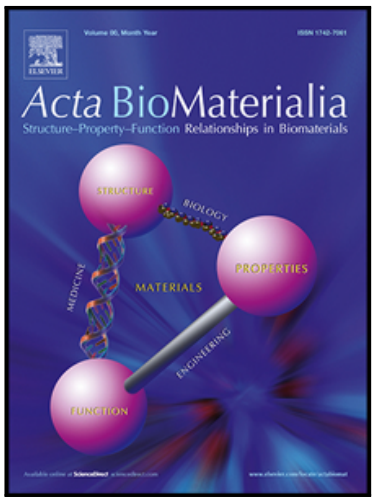

Biomimetic Tolerogenic Artificial Antigen Presenting Cells for Regulatory T Cell Induction

Kelly R. Rhodes , Randall A. Meyer , Justin Wang , Stephany Y. Tzeng , Jordan J. Green

PII: S1742-7061(20)30325-1
DOI: https://doi.org/10.1016/j.actbio.2020.06.004
Reference: ACTBIO 6766

To appear in: *Acta Biomaterialia*

Received date: 16 January 2020
Revised date: 29 May 2020
Accepted date: 2 June 2020

Please cite this article as: Kelly R. Rhodes , Randall A. Meyer , Justin Wang , Stephany Y. Tzeng , Jordan J. Green , Biomimetic Tolerogenic Artificial Antigen Presenting Cells for Regulatory T Cell Induction, *Acta Biomaterialia* (2020), doi: https://doi.org/10.1016/j.actbio.2020.06.004

Title:

Biomimetic Tolerogenic Artificial Antigen Presenting Cells for Regulatory T Cell Induction

Authors:

Kelly R. Rhodes[1,2,3], Randall A. Meyer[1,2,3], Justin Wang[1,2,3], Stephany Y. Tzeng[1,2,3], Jordan J. Green[1,2,3,4,5,6,7,*]

Affiliations:

1. Department of Biomedical Engineering, Johns Hopkins University School of Medicine, Baltimore, MD, 21231, USA.
2. Translational Tissue Engineering Center, Johns Hopkins University School of Medicine, Baltimore, MD, 21231, USA.
3. Institute for NanoBioTechnology, Johns Hopkins University School of Medicine, Baltimore, MD, 21231, USA.
4. Department of Chemical & Biomolecular Engineering, Johns Hopkins University, Baltimore, MD 21231, USA
5. Department of Materials Science and Engineering, Johns Hopkins University, Baltimore, MD, 21231, USA.
6. Department of Ophthalmology, Johns Hopkins University School of Medicine, Baltimore, MD, 21231, USA.
7. Department of Oncology, Sidney Kimmel Comprehensive Cancer Center and the Bloomberg~Kimmel Institute for Cancer Immunotherapy, Johns Hopkins University School of Medicine, Baltimore, MD, 21231, USA.

* To whom correspondence should be addressed: green@jhu.edu , (410) 614-9113
400 N Broadway, Smith Building Room 5017, Baltimore, MD, 21231, USA.

Graphical Abstract

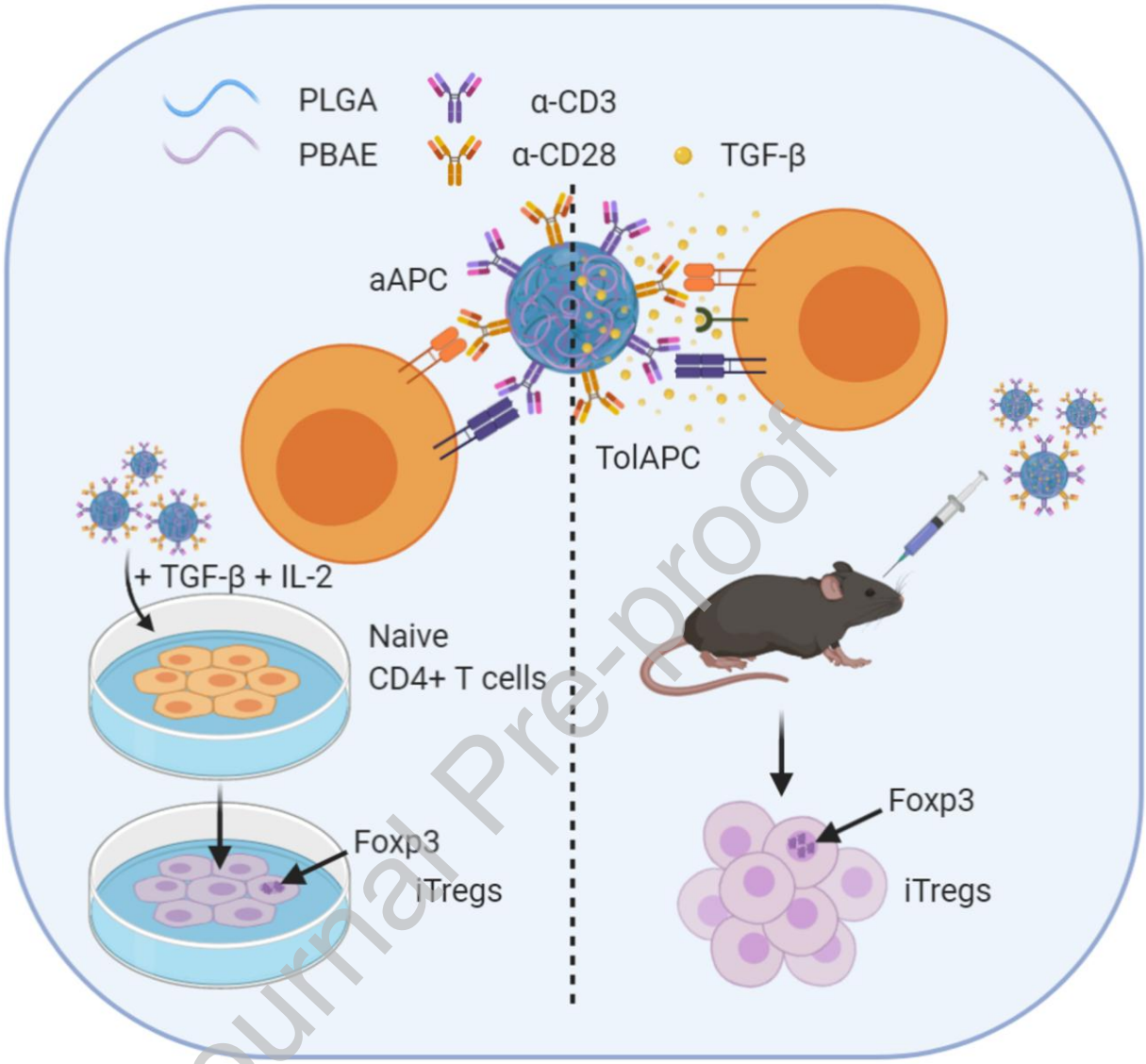

Abstract

Regulatory T cell (Treg)-based therapeutics are receiving increased attention for their potential to treat autoimmune disease and prevent transplant rejection. Adoptively transferred Tregs have shown promise in early clinical trials, but cell-based therapies are expensive and complex to implement, and "off-the-shelf" alternatives are needed. Here, we investigate the potential of artificial antigen presenting cells (aAPCs) fabricated from a blend of negatively charged biodegradable polymer (poly(lactic-co-glycolic acid), PLGA) and cationic biodegradable polymer (poly(beta-amino ester), PBAE) with incorporation of extracellular protein signals 1 and

2 and a soluble released signal 3 to convert naïve T cells to induced Foxp3+ Treg-like suppressor cells (iTregs) both *in vitro* and *in vivo* in a biomimetic manner. The addition of PBAE to the aAPC core increased the conjugation efficiency of signal proteins to the particle surface and resulted in enhanced ability to bind to naïve T cells and induce iTregs with potent suppressive function. Furthermore, PLGA/PBAE tolerogenic aAPCs (TolAPCs) supported the loading and sustained release of signal 3 cytokine TGF-β. A single dose of TolAPCs administered intravenously to C57BL/6J mice resulted in an increased percentage of Foxp3+ cells in the lymph nodes. Thus, PLGA/PBAE TolAPCs show potential as an "off-the-shelf" biomimetic material for tolerance induction.

Keywords: artificial antigen presenting cell, immunotherapy, regulatory T cell, tolerance, bioengineering, immunoengineering

Statement of Significance

Regulatory T cells (Tregs) are promising for basic research and translational medicine as they can induce tolerance and have the potential to treat autoimmune diseases such as type 1 diabetes and multiple sclerosis. As cell-based therapies are expensive and difficult to manufacture and implement, non-cellular methods of engineering endogenous Tregs are needed. The research reported here describes a new type of biomimetic particle, tolerogenic artificial antigen presenting cells (TolAPCs) fabricated from a blend of negatively charged biodegradable polymer, poly(lactic-co-glycolic acid), and positively charged biodegradable polymer, poly(beta-amino ester), along with key biomolecular signals: extracellularly presented protein signals 1 and 2 and a soluble released signal 3. These TolAPCs bind to naïve T cells and induce Foxp3+ Treg-like suppressor cells with potent suppressive function. In both *in vitro* and *in vivo* studies, it is shown that this non-cellular approach is useful to induce tolerance.

1. Introduction

Interest in regulatory T cells (Tregs) for antigen-specific immunotherapy stems from the discovery that a CD4+ CD25+ subset of T cells had the ability to suppress other cell types in response to self and non-self antigens.[1] As primary mediators of peripheral tolerance, Tregs work to regulate the immune system through several mechanisms targeting effector T cells and APCs. They are capable of directly destroying effector cells via cytolysis and suppressing effector cells through release of inhibitory cytokines, including TGF-β, IL-10, and IL-35, or

metabolic disruption via IL-2 starvation, transfer of cyclic adenosine monophosphate (cAMP), and adenosine release.[2, 3] Tregs can also inhibit dendritic cell maturation and induce dendritic cells to release indoleamine 2,3-dioxygenase (IDO) to suppress effector T cells. Because of their ability to induce tolerance through a variety of mechanisms, a growing number of therapies are being designed to target Tregs to establish tolerance toward specific antigens of interest. However, low autologous Treg numbers and defective function have been shown to contribute to a variety of autoimmune diseases, including type 1 diabetes (T1D), multiple sclerosis (MS), and systemic lupus erythematosus (SLE).[4] Strategies to increase Treg populations include expansion of Tregs, or *de novo* peripheral induction of Tregs from naïve T cells.

Although adoptive transfer of polyclonal Tregs shows promise in early-phase clinical trials for graft-versus-host disease[5, 6], organ transplantation,[7] and autoimmune disease,[8, 9] the rarity of Tregs in peripheral blood presents a major challenge to obtaining enough cells for transfer.[2] *In vitro* Treg expansions rely on high doses of IL-2 and have used antigen resenting cells (APCs) or anti-CD3/anti-CD28 beads.[10-12] However, Tregs are difficult to expand and may only be transiently functional following adoptive transfer, and strategies to directly modulate them *in vivo* are needed. Particle-based approaches are particularly versatile in their ability to deliver immunomodulatory factors and antigen specific signals in a targeted fashion to promote Tregs *in vivo*.[13] For example, Tostanoski *et al.* showed that biodegradable microparticles loaded with rapamycin and a myelin-derived peptide were shown to ameliorate experimental autoimmune encephalomyelitis (EAE) and reprogram the immune system toward a regulatory phenotype following a single injection into the inguinal lymph nodes of diseased mice.[14] Additionally, metallic nanoparticles functionalized with MHC Class I or II complexes show promise in reversing T1D and EAE in mice by expanding suppressive CD4+ and CD8+ T cells.[15]

In cases where preexisting Tregs are nonexistent or impaired, Treg induction has the potential to restore numbers and function and may be a more promising strategy than expansion of existing Tregs. However, there is a lack of effective technologies for antigen-specific Treg induction, particularly those that can be used to induce Tregs *in vivo*. Naïve T cells can be converted to Tregs by providing co-stimulation and TGF-β, the latter essential for transition to a regulatory phenotype.[4, 16] However, systemic administration of TGF-β causes significant off-target effects, necessitating localized delivery to T cells. Yang *et al.* demonstrated that tethering TGF-β to the surface of beads and natural APCs promotes Treg induction.[17] McHugh *et al*. showed that local TGF-β and IL-2 release in a controlled paracrine fashion from nanoparticles generated induced Tregs (iTregs) from naïve CD4+ T cells that were both functional and stable over time.[18] Controlled protein release to modulate T-cell responses has recently been explored in the context of artificial antigen presenting cell (aAPC) design to allow for precise modulation of T cell subsets coupled with presentation of essential T cell activation signals.[18-21] The term "aAPC" has been applied in many instances to describe a variety of cellular and acellular systems both specific and nonspecific, and synthesized from a variety of nondegradable and biodegradable materials.[22] We use the term aAPC from a reductionist standpoint—a 3D platform providing the minimum signals required to induce a T cell response. While newer generation aAPCs are being used to activate T cells, limited research has been conducted to design aAPCs to induce Tregs to promote immune tolerance.

One promising area of research is the use of different biodegradable polymers for the rigid aAPC core to increase their potency and "off-the-shelf" potential.[21] Although nondegradable materials have been investigated for *ex vivo* aAPC applications and poly(lactic-co-glycolic acid) (PLGA) is most commonly used as a biodegradable material for aAPCs construction, other biodegradable materials may possess beneficial properties for the fabrication of aAPCs. One important parameter governing T-cell activation is the surface density of signal proteins.[23] Close spacing is optimal but can be difficult to achieve with PLGA particles due to the low efficiency of certain conjugation strategies. To generate enhanced aAPCs, we utilize a novel core material consisting of a blend of PLGA and a hydrophobic poly(beta-amino ester) (PBAE). Rigid particles composed of a PLGA/PBAE blend have previously been used for intracellular nucleic acid delivery to immune cells [24], but have not been explored as a core material for aAPC technologies. Incorporating a hydrophobic, cationic polymer into the core of aAPCs has the potential to increase protein binding to the surface of the particles.[25] The addition of PBAE may enhance aAPC function and make it sufficiently potent for direct *in vivo* administration while also maintaining the advantages of PLGA in terms of biodegradability and biocompatibility.

Here, we investigated the ability of a biomimetic, biodegradable tolerogenic aAPC composed of a PLGA/PBAE blend to induce a population of Foxp3+ regulatory cells (iTregs) *in vitro* and *in vivo*. PLGA/PBAE aAPCs improved iTreg induction *in vitro* over PLGA aAPCs, showing the importance of biomaterial chemistry in aAPC design. iTregs were able to suppress the proliferation of naïve T cells. Finally, PLGA/PBAE aAPC loaded with TGF-β (TolAPC) promoted a regulatory T cell phenotype *in vivo*. These results demonstrate the effectiveness of PLGA/PBAE-based aAPC over PLGA aAPC for enhanced iTreg induction *in vitro* and the potential of a new TolAPC biomaterial system to improve T-cell polarization toward a regulatory phenotype *in vivo*.

2. Materials and Methods

2.1 Poly(beta-amino ester) synthesis and characterization

Poly(beta-amino ester) (PBAE) was synthesized using a two-step procedure. First, an acrylate-terminated base polymer was prepared through the Michael addition of 4,4'-trimethylenedipiperidine to 1,4-butanediol diacrylate at a 1.2:1 monomer ratio. The monomers were reacted neat and with stirring at 90°C for 24 hours to generate the base polymer. Next, the base polymer was dissolved in anhydrous tetrahydrofuran (THF) and reacted with an excess of end-capping monomer 1-(3-aminopropyl)-4-methylpiperazine at room temperature for 1 hour. The resulting end-capped PBAE polymer was purified with hexane, dried under vacuum, and stored at -20°C under nitrogen gas. The molecular weight of the PBAE was determined through gel permeation chromatography using an Ultrastyragel column with a molecular weight range of 500-30 kDa (Waters; Milford, MA) and a mobile phase of THF with 5% DMSO and 1% piperidine.

2.2 Tolerogenic artificial antigen presenting cell synthesis and characterization

2.2.1 Particle fabrication

Microparticles were made from poly(lactic-co-glycolic acid) (PLGA, acid-terminated, 50:50 lactide:glycolide ratio, MW 34,000-58,000 Da), purchased from Sigma Aldrich (St. Louis, MO), or a 75:25 w/w blend of PLGA and PBAE. To synthesize blank particles, 100 mg of polymer was dissolved in 5 mL dichloromethane (DCM) and homogenized into a 50-mL solution of 1% poly(vinyl alcohol) (PVA) by a T-25 digital ULTRA-TURRAX IKA tissue homogenizer at a speed of 5,000 rpm (IKA Works; Wilmington, NC). The resulting microparticle emulsion was then added to 100 mL of 0.5% PVA. To synthesize TGF-β-releasing particles for *in vivo* experiments, 50 mg of polymer was dissolved in 1 mL DCM. A 17.5 µL solution containing 2.5 µg recombinant mouse TGF-β and 1 mg bovine serum albumin (BSA) was added into the polymer solution and emulsified using a Misonix S-4000 probe sonicator operating at 12 W power 20% amplitude for 20 seconds (Qsonica; Newtown, CT). The resulting TGF-β/polymer emulsion was homogenized into 50 mL of 1% PVA 5,000 rpm, and the final emulsion was added into 100 mL of 0.5% PVA with stirring. The particles were allowed to harden for at least 4 hours. Particles were then washed three times in water with centrifugation at 3,000 × g, frozen, and lyophilized for later use.

2.2.2 Functionalization

PLGA and PLGA/PBAE microparticles were functionalized with proteins of interest using EDC/NHS chemistry, which couples primary amines on proteins of interest to carboxylic acid-terminated PLGA. Lyophilized particles were resuspended in 0.1 M MES buffer at pH 6.0 at a concentration of 2 mg/mL. An EDC/NHS solution consisting of 40 mg/mL EDC and 48 mg/mL NHS was added to each 2-mg batch of particles. Particles were activated at room temperature for 30 minutes. Following activation, particles were centrifuged at 5,000 × g for 5 minutes and resuspended in PBS at 2 mg/mL. Anti-mouse (clone: 145-2C11) or anti-human CD3 (clone: OTK3) (Biolegend; San Diego, CA) and CD28 (Bio X Cell; West Lebanon, NH) monoclonal antibodies were added at the following amounts, expressed as the mass of anti-CD3/anti-CD28 per mg of particles: 0.8 µg/ 1 µg (1/5×); 4 µg/ 5 ug (1×); and 20 µg/ 25 ug (5×). Particles were incubated with the protein overnight at 4°C to synthesize aAPCs. The following day, particles were washed 3 times with PBS and used immediately.

2.2.3 Characterization

Microparticles were imaged and sized using scanning electron microscopy (SEM). Lyophilized particles were spread onto aluminum tacks mounted with double-sided carbon tape. Excess particles were removed from the tack with an air gun. Samples were sputter-coated with a 20-nm layer of gold/palladium and imaged on a LEO FESEM (Zeiss). Particle size was measured by image analysis in ImageJ. Zeta potential was measured using a ZetaSizer (Malvern).

To assess TGF-β release from PLGA and PLGA/PBAE microparticles, lyophilized particles were resuspended in PBS at 10 mg/mL and incubated at 37°C. Supernatants were collected at various timepoints by centrifuging samples at 5,000 × g and were replaced with fresh PBS. TGF-β in the supernatant was measured using a sandwich ELISA (Biolegend).

To quantify the amount of protein on the surface of aAPCs, particles were conjugated with 1/5×, 1×, or 5× AlexaFluor 488-labeled anti-CD3 (clone: 145-2C11) and allophycocyanin-labeled anti-CD28 (clone: 37.51) using EDC/NHS chemistry as described above. After conjugation, aAPCs were washed three times with PBS, and fluorescence was evaluated using a BioTek Synergy 2 plate reader (Biotek; Winooski, VT). Particles were conjugated under sterile conditions prior to use *in vitro* and *in vivo*, and all reagents used in particle synthesis and preparation were tested for endotoxin. The mass of protein on the particle was calculated against a standard curve generated from known amounts of labeled protein to evaluate protein conjugation efficiency. To measure surface protein retention over time, aAPCs were incubated in PBS at 37°C for 7 days. Supernatants were collected at various timepoints and analyzed via plate reader.

2.3 Isolation of Naïve CD4+ CD25- T cells

All mice were maintained according to the Johns Hopkins University Institutional Animal Care and Use Committee. Male C57BL/6J mice aged 8-12 weeks were sacrificed, and their spleens were dissected and homogenized though a cell strainer. CD4+ CD25- cells were isolated using a CD4+ T-cell isolation kit (Miltenyi Biotec; Auburn, CA). Briefly, cells were incubated with a cocktail of biotin-conjugated antibodies to deplete non CD4+ T cells, and a biotinylated anti-mouse CD25 monoclonal antibody (clone: PC61; Biolegend) was added at 1 µL per 10^7 cells to deplete CD25+ cells. Cells were then labelled with anti-biotin-conjugated magnetic micro-beads and magnetically separated to obtain an enriched population of CD4+ CD25- T cells.

2.4 *in vitro* aAPC/T-cell binding assay

PLGA and PLGA/PBAE microparticles were synthesized as previously described except the initial DCM solution also included 10 µg of Vybrant DiD Cell-Labeling Solution (Thermo Fisher Scientific; Waltham, MA). Control PLGA and PLGA/PBAE aAPCs were surface-conjugated with an anti-human CD3 monoclonal antibody (clone: OTK3; Biolegend). C57BL/6J splenocytes or CD4+ T cells were labeled with Vybrant Cell Tracker carboxyfluorescein succinyl ester (CFSE) (Life Technologies; Grand Island, NY) dye according to the manufacturer's protocol. Cells were incubated with aAPCs at a concentration of 0.05 or 0.01 mg aAPCs/50,000 cells for 1 hour at 37°C. Prior to confocal imaging the cells were gently washed 3 times with PBS to remove unbound particles. Confocal micrographs were obtained using a Zeiss 710 LSM (Carl Zeiss Microscopy; Jena, Germany). aAPC/T-cell binding was assessed on an Accuri C6 Flow Cytometer (BD Biosciences; San Jose, CA). Splenocyte samples were also stained with Brilliant Violet 421-labelled anti-CD3 (clone: 145-2C11; Biolegend). CFSE and DiD double-positive events were considered instances of binding. DiD geometric mean fluorescence intensity (MFI) of CFSE+ cells was also used to evaluate the extent of aAPC binding to cells. DiD MFI values were normalized to control samples with cells and unconjugated particles to account for differences in fluorescence between PLGA and PLGA/PBAE particles.

2.5 *in vitro* aAPC-mediated iTreg induction

C57BL/6J cells were incubated with aAPCs at 1, 0.1, 0.01, or 0.001 mg/mL in RPMI media supplemented with L-glutamine, non-essential amino acids, vitamin solution, sodium pyruvate, β-mercaptoethanol, 10% FBS, ciprofloxacin, and 400 U/mL human IL-2. TGF-β was added at 5

ng/mL. After five days, cells were stained with CFSE according to the manufacturer's protocol. CFSE-labeled cells were then fixed, permeabilized, and stained for Forkhead Box Protein 3 (Foxp3) using a Foxp3 staining kit (Thermo Fisher Scientific). Foxp3 expression was assessed through flow cytometry analysis on an Accuri C6 Flow Cytometer. For additional phenotype studies, cells were also stained with antibodies against CD4 (RM4-5) – AF 488, CD25 (PC61) - PE, Foxp3 (FJK-16s) – Pacific Blue, CD39 (Duha59) - APC, and CD73 (TY/11.8) – APC/Fire 750. For human iTreg induction studies, naïve CD4+ human T cells were purchased commercially (Zen-Bio; Research Triangle Park, NC) and incubated with aAPCs as previously described. After five days, cells were stained for CD4 (SK3) – PE, CD25 (M-A251) – PE/Cy7, and FOXP3 (PCH101) – Pacific Blue and analyzed using flow cytometry.

2.6 Cytokine secretion analysis

iTregs were induced with PLGA/PBAE aAPCs in the presence or absence of exogenous TGF-β as previously described. Culture supernatants were harvested and relative levels of cytokines were determined using a Proteome Profiler Mouse Cytokine Array Kit (R&D Systems; Minneapolis, MN). ImageJ was used to analyze the pixel density in spots of the array, and the averaged background signal from negative control spots was subtracted.

2.7 Quantification of *foxp3*

iTregs were induced with PLGA/PBAE aAPCs in the presence or absence of exogenous TGF-β. Cells were then harvested and DNA was extracted and sent to EpigenDx (Hopkintown, MA) for pyrosequencing to determine percent methylation of various CpG motifs within the *foxp3* locus.

2.8 iTreg stability assay

iTregs were induced with PLGA/PBAE aAPCs in the presence or absence of exogenous TGF-β. After induction, cells were washed and plated at 100,000 cells/ well in media with 40 U/mL IL-2. Media was changed every two days, and on Days 2 and 7 cells were stained for CD4, CD25, and Foxp3 and analyzed using flow cytometry.

2.9 *In vitro* induced-iTreg suppression assay

The functionality of induced iTregs was verified through their ability to suppress the proliferation of naïve CD4+ T cells. iTregs were induced for five days with 0.1 mg/mL PLGA or PLGA/PBAE aAPCs in the presence of TGF-β (5 ng/mL) and IL-2 (400 U/mL), or with cytokines only as a negative control. After five days, suppressor populations were harvested. The responder population consisted of CD4+ CD25- T cells isolated from Thy1.1 C57BL/6J mice and labeled with CFSE as previously described. Suppressor and responder populations were mixed at 1:1, 1:2, 1:4, 1:8 or 0:1 ratios in a 96-well plate (50,000 responder cells per well). Anti-CD3/anti-CD28 Dynabeads were added to each well at a 1:2 bead/responder cell ratio. After 3 days, cells were stained for Thy1.1 (OX-7) – APC and analyzed using flow cytometry. Proliferation of responder cells was assessed through CFSE dilution. Since the CFSE dye is diluted in half with each cell division, each generation of cells is defined by a distinct peak on the CFSE histogram. To calculate the percent suppression, the division index (DI), or the average number of divisions undergone by responder cells, was calculated in FlowJo, then the following

equation was used: 100 – (DI_{sample} / $DI_{control}$) x 100, where the control is proliferation of responder cells in the absence of suppressors.[26]

2.10 *In vivo* TolAPC-mediated iTreg induction

The effectiveness of TGF-β-loaded TolAPCs at polarizing CD4+ T cells toward a regulatory phenotype *in vivo* was investigated. TGF-β-releasing TolAPCs were injected intravenously into C57BL/6J mice. Control mice received either TGF-β-loaded, unconjugated PLGA/PBAE particles or no treatment. After five days, mice were sacrificed and their spleens were harvested and lymph nodes (inguinal, axillary, and cervical) were harvested and pooled. Single cell suspensions were generated through cell straining, and cells were stained for CD4 and Foxp3. Following staining, cells were analyzed using flow cytometry.

2.11 Statistical Methods

Multiple comparisons were made using one-way or two-way ANOVA with Tukey's or Sidak's post-tests when comparing across groups. Two-tailed Student's *t* tests were used when comparing two groups. All graphs show mean and error bars that represent SEM. All *n* values are shown in graphs or present within figure legends. For data in Figure 1, the Mann-Whitney Test was used to compare two groups, because sample sizes were insufficient to determine normality. All statistical analysis was performed using GraphPad Prism software.

3. Results

3.1 aAPC fabrication and characterization

After synthesis via two sequential Michael addition reactions (Figure 1A), the resulting PBAE had a number average molecular weight (Mn) of about 28 kDa and weight average molecular weight (Mw) of about 137 kDa. PLGA or PLGA/PBAE aAPCs were surface-functionalized with anti-CD3 as signal 1 and anti-CD28 for co-stimulation. We evaluated PLGA and PLGA/PBAE aAPC size and morphology using SEM. SEM images revealed that PLGA and PLGA/PBAE particles were spherical (Figure 1B). Through image analysis, PLGA and PLGA/PBAE particles were determined to be similar in size, with an average diameter of approximately 3 μm (Figure 1C). This size enables aAPCs to mimic the biological length scale of the natural APC/T cell interaction while being small enough for systemic administration without pulmonary embolism. PLGA and PLGA/PBAE particles also had similar zeta potentials of -2.47 ± 2.84 and -2.77 ± 2.61 mV, respectively (Figure 1D).

aAPCs functionalized with anti-CD3 and anti-CD28 nonspecifically stimulate T cells, so TGF-β must be added exogenously or loaded into the particle core to fabricate tolerogenic aAPCs (TolAPCs) to polarize CD4+ T cells toward a regulatory phenotype *in vivo*. TGF-β release over time was quantified using an ELISA. PLGA and PLGA/PBAE particles degraded over the course of a month. Total TGF-β release from PLGA and PLGA/PBAE particles was 1.5 and 0.26 ng/mg particles, respectively (Figure 1E).

We compared the surface protein content of PLGA and PLGA/PBAE aAPCs across three different doses of anti-CD3 and anti-CD28 added into the conjugation media. Fluorescently labeled anti-CD3 and anti-CD28 were conjugated to the surface of particles, and the fluorescence intensity measurements were used to quantify the protein on the surface of newly synthesized aAPCs. PLGA/PBAE aAPCs were found to have significantly more bound anti-CD3 and anti-CD28 than PLGA aAPCs when 1/5, 1, or 5× protein doses were added to the conjugation media (Figure 1F-G). Conjugated protein is also stably presented on aAPCs, with 86% protein remaining on PLGA/PBAE and 67% on PLGA APCs after particles were incubated for 7 days in PBS at 37°C (Figure 1H-I). Since PLGA/PBAE particles conjugate protein more efficiently than PLGA particles, less protein is needed to synthesize PLGA/PBAE aAPCs.

3.2 PLGA/PBAE aAPCs bind more frequently to naïve CD4+ T cells

aAPC function is based on the synthetic particle's ability to target and interact efficiently with biological T cells to present the necessary activation signals. T-cell activation is dependent on aAPC binding and signal presentation across the particle/cell interface. We compared the ability of PLGA and PLGA/PBAE aAPCs to bind target cells. A hydrophobic dye was encapsulated in the core of aAPCs during particle synthesis to generate fluorescent aAPCs. Fluorescent PLGA and PLGA/PBAE aAPCs were functionalized according to the previously described methods. Control aAPCs were surface-functionalized with anti-human CD3 antibody with no specific binding to the mouse TCR. PLGA and PLGA/PBAE aAPCs were incubated with CFSE-labeled CD4+ CD25- T cells at 37°C for one hour. Binding was visualized using confocal microscopy (Figure 2A). Images show that PLGA/PBAE aAPCs bind to T cells more frequently than PLGA aAPCs and control aAPCs. The fraction of bound cells was determined by flow cytometry by gating on CFSE and DiD double-positive events, which indicate colocalization of aAPCs and T-cells (Figure 2B-C). Background signal was determined from samples of blank PLGA and PLGA/PBAE particles and cells and was subtracted from calculated binding values. No significant binding of control aAPCs with surface-bound anti-human CD3 was observed. The percentage of T cells bound to PLGA/PBAE aAPCs was 30 ± 2 %, compared to 8 ± 2 % bound to PLGA aAPCs at the highest particle dose tested (Figure 2B). The MFI of PLGA/PBAE aAPC binding events was 4.5-fold higher than that of PLGA aAPC binding events, indicating a higher average number of bound particles per T cell (Figure 2D-E). We also investigated the binding specificity of PLGA and PLGA/PBAE aAPCs for CD3+ T cells using flow cytometry (Supplementary Figure 1). PLGA/PBAE aAPCs show significantly higher binding to CD3+ T cells over CD3- splenocytes and increased binding to CD3+ T cells compared to PLGA aAPC. Relatively low binding of PLGA aAPCs to CD3+ and CD3- splenocytes and modest specificity for CD3+ cells was observed (Supplementary Figure 1).

3.3 PLGA/PBAE aAPCs induce more iTregs *in vitro*

We tested the potential of our PLGA and PLGA/PBAE aAPCs to convert iTregs from naïve CD4+ cells *in vitro*. PLGA and PLGA/PBAE aAPCs with 1/5×, 1×, and 5× surface-bound signal protein densities were incubated with CD4+ CD25- T cells for 5 days in the presence of TGF-β and IL-2 and then analyzed for iTreg induction by flow cytometry. We sought to optimize the surface protein density and aAPC dose for maximum conversion to the iTreg phenotype and

compare the ability of PLGA/PBAE and PLGA aAPCs to induce iTregs. We observed dose-dependent iTreg induction after incubation with aAPCs (Figure 3). PLGA/PBAE aAPCs with all three tested surface protein densities outperformed PLGA aAPCs, generating significantly larger percentages of Foxp3+ cells at 1, 0.1, and 0.01 mg/mL aAPC doses. The greatest separation between PLGA and PLGA/PBAE aAPC performance occurred at a 0.1 mg/mL dose with aAPCs conjugated with 1× surface protein, so we used this protein density and aAPC dose for later experiments. We also used PLGA and PLGA/PBAE aAPCs surface-conjugated with anti-human CD3 and CD28 antibodies to induce a CD25+ Foxp3+ population from naïve human CD4+ T cells in the presence of exogenous TGF-β and IL-2 (Supplementary Figure 2A). We found that PLGA and PLGA/PBAE aAPC were able to induce about 35% and 40% human CD25+ FOXP3+ cells, respectively, at a 0.1 mg/mL dose. PLGA/PBAE aAPCs were more efficient than PLGA at a 0.01 mg/mL dose, inducing about 31% CD25+ FOXP3+ cells compared to 20.0% (Supplementary Figure 2B). PLGA/PBAE also increased CD25 expression compared to PLGA aAPCs at both doses tested (Supplementary Figure 2C).

3.4 iTregs exhibit a suppressive phenotype

Tregs are characterized by their potent suppressive capabilities. One important mechanism of Treg-mediated suppression is the production adenosine, which downregulates NF-κB activation in effector T cells and acts on Tregs to further enhance their immunosuppressive capacity. CD39 and CD73 are involved in the conversion of ATP to adenosine and are highly expressed on the surface of Tregs.[27-29] We thus sought to characterize CD39 and CD73 expression on iTregs. We induced iTregs using PLGA or PLGA/PBAE aAPCs in the presence or absence of exogenous TGF-β. Representative flow plots reveal that in the absence of TGF-β, about 97% of PLGA/PBAE TolAPC-induced cells were CD25+, while only 34% of PLGA TolAPC-induced cells were CD25+ (Figure 4A). In the presence of TGF-β, PLGA/PBAE aAPCs were quite efficient at generating iTregs, as evidenced by over 70% of the cells expressing CD25 and Foxp3, while PLGA aAPCs were less efficient, only inducing about 13% CD25+Foxp3+ cells (Figure 4B-C). In the presence of TGF-β, a majority of iTregs co-expressed CD39 and CD73, with PLGA/PBAE aAPC-induced iTregs demonstrating the highest levels of co-expression (Figure 4D). PLGA/PBAE aAPC-induced iTregs exhibited significantly higher CD39 expression compared to PLGA aAPC-induced iTregs and CD25+ cells induced in the absence of TGF-β, and both PLGA and all iTregs showed higher levels of CD73 expression compared to control CD25+ cells (Figure 4E-F). To further investigate the signature of iTregs compared to activated CD4+ T cells, we also analyzed cytokine secretion of iTregs and control T cells induced by PLGA/PBAE aAPCs in the presence or absence of TGF-β using a Proteome Profiler Mouse Cytokine Array Kit. We found that iTregs secreted lower amounts of several inflammatory cytokines compared to control T cells (Supplementary Figure 3).

3.5 iTregs have a partially demethylated Foxp3 locus and are relatively unstable *in vitro*

Demethylation of the Foxp3 locus leads to stable Foxp3 expression in Tregs. It has been shown that Tregs induced by TGF-β *in vitro* have a highly methylated Treg-cell-specific demethylated region (TSDR) despite high Foxp3 expression.[30] Despite this typical signature of methylated TSDRs in Tregs induced *in vitro*, we found reduced methylation of the TSDR in T cells induced

with PLGA/PBAE aAPCs supplemented with exogenous TGF-β compared to those induced without TGF-β (Supplementary Figure 4). We also evaluated the stability of iTregs induced by PLGA/PBAE aAPCs in the presence or absence of exogenous TGF-β. After induction, induced populations were cultured for an additional 7 days with 40 U/mL IL-2. In agreement with others,[31, 32] we found that Foxp3 expression in iTregs decreases over time following induction, with about 20% Foxp3+ cells remaining after 7 days. Foxp3 expression remains quite low for populations induced in the absence of TGF-β (Supplementary Figure 5).

3.6 iTregs suppress proliferation of CD4+ T cells

We investigated the ability of iTregs to suppress T-cell proliferation in order to verify the suppressive potential of our aAPCs. First, iTreg induction was carried out over five days as previously described, using PLGA and PLGA/PBAE aAPCs at a 0.1 mg/mL dose. After the induction period, the suppressor populations were harvested and incubated at titrated doses with CFSE-labeled Thy1.1+ responder cells and anti-CD3/anti-CD28 Dynabeads for three days. On the third day, samples were analyzed using flow cytometry (Figure 5A). Foxp3 expression in the suppressor population was assessed before incubation with responder cells (Figure 5B). Dose-dependent suppression of responder T cells was observed for aAPC-induced iTregs (Figure 5C), with significantly less responder proliferation in the presence of PLGA/PBAE aAPC-induced suppressor populations than in the presence of PLGA aAPC-induced suppressor populations (Figure 5D).

3.7 PLGA/PBAE TolAPCs increase Foxp3+ levels *in vitro* and *in vivo*

We sought to evaluate the potential of aAPCs to polarize the endogenous T-cell repertoire towards a regulatory phenotype *in vivo*. We encapsulated TGF-β in the core of PLGA and PLGA/PBAE aAPCs to generate TolAPCs. TolAPCs were first used to induce Tregs *in vitro* for 4 days in the presence of IL-2. (Figure 6A). PLGA/PBAE TolAPC induced more iTregs than PLGA TolAPC at a 0.5 mg/mL dose. A 2 mg dose of TGF-β-loaded TolAPCs or TGF-β-loaded unconjugated particles was administered intravenously to mice. Five days later, animals were sacrificed and T cells from the spleens and lymph nodes were stained for CD4 and Foxp3 expression (Figure 7A). Cells were analyzed using flow cytometry, and Foxp3+ cells were quantified as a percentage of CD4+ cells (Figure 7B). Administration of PLGA/PBAE TolAPCs led to Foxp3+ populations of 14.8 ± 2.4 % within the CD4+ population in the spleen and 14.1 ± 1.1 % in the lymph nodes, the latter a 20 % relative increase over control mice (Figure 7C-D).

4. Discussion

Treg-based therapies are a promising approach to treat autoimmune disease and prevent transplant rejection, although a major barrier to their use is the lack of efficient expansion and induction techniques.[2] Particle-based systems represent an “off-the-shelf” approach to establishing immune tolerance, and may be more easily translated than cell-based therapies. Recent advancements highlight the potential of biomimetic and biodegradable artificial antigen presenting cells (aAPCs) as a clinical immunotherapy. However, they are typically used in the context of adoptive transfer and have not been used to directly stimulate the endogenous T-cell repertoire. Furthermore, their application for immune tolerization is limited. The purpose of this

work is to evaluate the ability of aAPCs constructed from a novel hybrid polymeric core material to induce a population of suppressor cells that can suppress an immune response for immunomodulatory or immune tolerance applications.

Here, we have developed and characterized a tolerogenic aAPC with a novel core material that enhances surface protein presentation and supports the incorporation of a third immunomodulatory signal, and used these TolAPCs to convert naïve T cells into iTregs. Related PLGA-based aAPCs have been shown to effectively stimulate T cells against tumor-specific antigens in adoptive transfer cancer models, and their potential has been demonstrated through their ability to encapsulate and release cytokines in a controlled manner due to their biodegradability.[18, 20] We blended PLGA with an additional polymer, PBAE, to enhance extracellular protein presentation and aAPC potency. T-cell activation is dependent on surface protein spacing, with close packing of signaling ligands being optimal. A density of 1,000 anti-CD3 molecules/μm^2 has previously been shown to better activate CD4+ T cells compared to lower densities.[33] We showed that the addition of PBAE to the aAPC core allowed protein addition to the particle surface at a higher density than PLGA alone. Protein presentation was shown to be stable, with over 80% protein retention on the surface of PLGA/PBAE aAPCs after 7 days. The incorporation of PBAE, a hydrophobic and cationic polymer, may increase nonspecific adsorption of protein to the polymer surface, as it has been previously shown that protein can coat the surface of hydrophobic polystyrene particles in the absence of other chemically active reagents.[25] Increased surface coating and improved protein retention may allow PLGA/PBAE particles to achieve a more optimal surface protein density than that of PLGA particles.

Incorporation of PBAE in the aAPC core also enhanced aAPC binding to naïve CD4+ T cells, another critical aspect determining aAPC efficacy.[34] PLGA/PBAE aAPCs bound a higher percentage of CD4+ T cells than PLGA aAPCs and control aAPCs displaying an anti-human CD3 antibody. PLGA/PBAE aAPCs also showed enhanced binding and greater specificity for CD3+ cells within a mixed splenocyte population. More frequent binding events for PLGA/PBAE may potentially be attributed to the increased signal protein density on PLGA/PBAE aAPCs, since higher densities correlate to increased binding to T cells.[34]

PLGA/PBAE aAPCs were further able to robustly induce iTregs from naïve CD4+ splenocytes *in vitro*, outperforming PLGA aAPCs and soluble factors over a range of surface-bound signal protein densities tested. These effects are likely due in part to increased surface protein on PLGA/PBAE aAPCs. Induction levels were highest when a 1× protein dose (4 µg anti-CD3 and 5 µg anti-CD28 per mg particles) was conjugated to PLGA/PBAE particles during aAPC synthesis, compared to a 5× or 1/5× dose (Figure 3). Meanwhile, low levels of induction were observed for PLGA aAPCs, and the best performance was observed at a 5× protein dose. Increased protein density correlates with improved iTreg induction potential. For PLGA/PBAE aAPCs, a high protein dose during conjugation (20 µg anti-CD3 and 25 µg anti-CD28 per mg particles) may be too immunostimulatory, thereby decreasing the efficiency of iTreg induction. In addition to altering the overall surface protein density, robust stimulatory capacity of

PLGA/PBAE aAPCs can potentially be modulated by increasing the ratio of signal 1 to signal 2 proteins to favor iTreg formation.

To demonstrate feasibility and translatability of our approach, we also showed that PLGA and PLGA/PBAE aAPCs can be used to induce a CD25+ FOXP3+ population from naïve human CD4+ cells (Supplementary Figure 2). PLGA and PLGA/PBAE aAPCs induced relatively similar levels of FOXP3+ cells at a 0.1 mg/ mL dose, although the same dose added to murine cells typically leads to a large difference in the efficacy of PLGA and PLGA/PBAE aAPCs. At a tenfold lower dose, PLGA/PBAE aAPC treatment resulted in significantly more FOXP3+ cells compared to PLGA aAPCs. Future studies should optimize aAPCs and TolAPCs for human iTreg induction, evaluate the extent of activation induced FOXP3, and investigate the suppressive capacity of iTregs to demonstrate the therapeutic potential of aAPCs.

After inducing iTregs from mouse naïve CD4+ T cells, we performed additional phenotypic analysis. PLGA/PBAE aAPC-induced iTregs showed increased co-expression of CD39 and CD73 compared to PLGA aAPC, two receptors involved in the conversion of ATP to adenosine (Figure 4). Adenosine downregulates NF-κB activation in effector T cells and acts on Tregs to further enhance their immunosuppressive capacity. CD4+ T cells activated by aAPCs in the absence of TGF-β showed little Foxp3, CD39, and CD73 expression, high levels of CD25, and increased secretion of several inflammatory cytokines compared to iTregs (Figure 4, Supplementary Figure 3). Notably, PLGA/PBAE aAPCs induced much higher levels of CD25 than PLGA aAPCs regardless of TGF-β, likely due to the higher density of anti-CD3 and anti-CD28 on the surface of PLGA/PBAE aAPCs compared to PLGA aAPCs.

Typically, Tregs induced *in vitro* typically have a high degree of Foxp3 methylation, and are widely accepted as fairly unstable and plastic.[35, 36] We found iTregs contained a partially demethylated Foxp3 locus, and observed about 20% Foxp3+ cells remaining after 7 days in culture following induction (Supplementary Figures 4-5). Stability of iTregs is an important challenge that should be addressed to maximize the therapeutic potential of these cells. However, it has been shown that Treg induction *in vivo* can lead to more stable Tregs compared to *in vitro* induction.[35, 37] Additionally, administration of IL-2 *in vivo* following adoptive transfer of Tregs induced *in vitro* can stabilize Foxp3 expression and preserve suppressor function, which is a promising way to address the inherent instability of iTregs.[31]

aAPC-induced suppressor populations were able to suppress the proliferation of naïve CD4+ T cells *in vitro* in a dose-dependent manner. Significantly less responder proliferation was observed in PLGA/PBAE conditions compared to PLGA at the three highest suppressor: responder ratios tested (Figure 6D). PLGA/PBAE aAPC-induced suppressor populations almost completely suppressed the proliferation of responder cells when cultured at a 1:1 ratio, while populations induced by PLGA aAPCs or soluble cytokines demonstrated less potent suppressive activity.

Finally, we sought to study the effectiveness of PLGA/PBAE aAPCs at inducing iTregs directly *in vivo*. We have previously demonstrated that PLGA micro-aAPC have a half-life of 11.6 minutes in circulation, and can be detected in the spleen at least 48 hours after systemic

administration.[38] Since TGF-β is necessary for the development of the iTreg phenotype, we encapsulated it within our aAPCs to achieve sustained, local release. Local release of TGF-β has previously been shown to mediate more effective iTreg conversion than equivalent soluble concentrations.[18] We synthesized TolAPCs loaded with TGF-β and demonstrated sustained release from PLGA and PLGA/PBAE TolAPCs and iTreg induction *in vitro* (Figure 1, Figure 6). A single dose of PLGA/PBAE TolAPCs administered intravenously was sufficient to modestly bias the T-cell repertoire in the lymph nodes toward a regulatory phenotype *in vivo* compared mice receiving no treatment (Figure 7). The same trend was observed in the spleen. PLGA TolAPCs were unable to significantly bias the repertoire towards iTregs despite their ability to release more TGF-β than PLGA/PBAE TolAPCs.

Together these results demonstrate that the addition of PBAE to the aAPC core confers superior properties to the aAPC, including increased surface protein density, enhanced binding to naïve T cells, and more efficient T-cell activation and polarization, as illustrated by their ability to more effectively induce conversion of naïve T cells to iTregs. Biodegradable PLGA/PBAE particles that incorporate both extracellular presented proteins as well as soluble released proteins may be promising for multiple immunomodulation applications.

5. Conclusions

We have developed a biomimetic biodegradable polymeric artificial antigen presenting cell capable of polarizing T cells toward a regulatory phenotype. The addition of PBAE to the core material of PLGA-based aAPCs increases protein conjugation efficiency to particulate cores and enhances the ability of aAPCs to interact with T cells and convert them to functional iTregs *in vitro*. These biodegradable aAPCs support the sustained release of signal 3 cytokine TGF-β. TGF-β-loaded PLGA/PBAE TolAPCs were shown to increase the frequency of iTregs *in vivo* following a single intravenous injection. PLGA/PBAE may be a promising material for the construction of aAPC with potent immunomodulatory capacity when administered directly *in vivo*.

Acknowledgements

Funding: This work was supported by the National Institutes of Health (NIH) (P41EB028239 and R01CA195503) and the Juvenile Diabetes Research Foundation (1-PNF-2019-782-S-B). K.R. and R.M. also thank the National Science Foundation (DGE-1232825) and the NIH (F31CA214147) respectively for fellowship support. The authors thank the Bloomberg~Kimmel Institute for Cancer Immunotherapy for support.

Data Availability

The raw/processed data required to reproduce these findings cannot be shared at this time as the data also forms part of an ongoing study.

Declaration of interests

The authors declare that they have no known competing financial interests or personal relationships that could have appeared to influence the work reported in this paper.

References

[1] S. Sakaguchi, N. Sakaguchi, M. Asano, M. Itoh, M. Toda, Immunologic self-tolerance maintained by activated T cells expressing IL-2 receptor alpha-chains (CD25). Breakdown of a single mechanism of self-tolerance causes various autoimmune diseases, J Immunol 155(3) (1995) 1151-64.
[2] M. Gliwinski, D. Iwaszkiewicz-Grzes, P. Trzonkowski, Cell-Based Therapies with T Regulatory Cells, BioDrugs 31(4) (2017) 335-347.
[3] D.A. Vignali, L.W. Collison, C.J. Workman, How regulatory T cells work, Nat Rev Immunol 8(7) (2008) 523-32.
[4] S.A. Long, J.H. Buckner, CD4+FOXP3+ T regulatory cells in human autoimmunity: more than a numbers game, J Immunol 187(5) (2011) 2061-6.
[5] A. Theil, S. Tuve, U. Oelschlagel, A. Maiwald, D. Dohler, D. Ossmann, A. Zenkel, C. Wilhelm, J.M. Middeke, N. Shayegi, K. Trautmann-Grill, M. von Bonin, U. Platzbecker, G. Ehninger, E. Bonifacio, M. Bornhauser, Adoptive transfer of allogeneic regulatory T cells into patients with chronic graft-versus-host disease, Cytotherapy 17(4) (2015) 473-86.
[6] P. Trzonkowski, M. Bieniaszewska, J. Juscinska, A. Dobyszuk, A. Krzystyniak, N. Marek, J. Mysliwska, A. Hellmann, First-in-man clinical results of the treatment of patients with graft versus host disease with human ex vivo expanded CD4+CD25+CD127- T regulatory cells, Clin Immunol 133(1) (2009) 22-6.
[7] E.K. Geissler, The ONE Study compares cell therapy products in organ transplantation: introduction to a review series on suppressive monocyte-derived cells, Transplant Res 1(1) (2012) 11.
[8] J.A. Bluestone, J.H. Buckner, M. Fitch, S.E. Gitelman, S. Gupta, M.K. Hellerstein, K.C. Herold, A. Lares, M.R. Lee, K. Li, W. Liu, S.A. Long, L.M. Masiello, V. Nguyen, A.L. Putnam, M. Rieck, P.H. Sayre, Q. Tang, Type 1 diabetes immunotherapy using polyclonal regulatory T cells, Sci Transl Med 7(315) (2015) 315ra189.
[9] ClinicalTrials.gov. (Accessed 27 August 2019.
[10] Q. Tang, K.J. Henriksen, M. Bi, E.B. Finger, G. Szot, J. Ye, E.L. Masteller, H. McDevitt, M. Bonyhadi, J.A. Bluestone, In vitro-expanded antigen-specific regulatory T cells suppress autoimmune diabetes, J Exp Med 199(11) (2004) 1455-65.
[11] S. Yamazaki, T. Iyoda, K. Tarbell, K. Olson, K. Velinzon, K. Inaba, R.M. Steinman, Direct expansion of functional CD25+ CD4+ regulatory T cells by antigen-processing dendritic cells, J Exp Med 198(2) (2003) 235-47.
[12] D. Sarkar, M. Biswas, G. Liao, H.R. Seay, G.Q. Perrin, D.M. Markusic, B.E. Hoffman, T.M. Brusko, C. Terhorst, R.W. Herzog, Ex Vivo Expanded Autologous Polyclonal Regulatory T Cells Suppress Inhibitor Formation in Hemophilia, Mol Ther Methods Clin Dev 1 (2014).
[13] E. Ben-Akiva, S. Est Witte, R.A. Meyer, K.R. Rhodes, J.J. Green, Polymeric micro- and nanoparticles for immune modulation, Biomater Sci 7(1) (2018) 14-30.
[14] L.H. Tostanoski, Y.C. Chiu, J.M. Gammon, T. Simon, J.I. Andorko, J.S. Bromberg, C.M. Jewell, Reprogramming the Local Lymph Node Microenvironment Promotes Tolerance that Is Systemic and Antigen Specific, Cell Rep 16(11) (2016) 2940-2952.
[15] S. Tsai, A. Shameli, J. Yamanouchi, X. Clemente-Casares, J. Wang, P. Serra, Y. Yang, Z. Medarova, A. Moore, P. Santamaria, Reversal of autoimmunity by boosting memory-like autoregulatory T cells, Immunity 32(4) (2010) 568-80.

[16] W. Chen, W. Jin, N. Hardegen, K.J. Lei, L. Li, N. Marinos, G. McGrady, S.M. Wahl, Conversion of peripheral CD4+CD25- naive T cells to CD4+CD25+ regulatory T cells by TGF-beta induction of transcription factor Foxp3, J Exp Med 198(12) (2003) 1875-86.
[17] E.Y. Yang, J.P. Kronenfeld, K.M. Gattas-Asfura, A.L. Bayer, C.L. Stabler, Engineering an "infectious" T(reg) biomimetic through chemoselective tethering of TGF-beta1 to PEG brush surfaces, Biomaterials 67 (2015) 20-31.
[18] M.D. McHugh, J. Park, R. Uhrich, W. Gao, D.A. Horwitz, T.M. Fahmy, Paracrine co-delivery of TGF-beta and IL-2 using CD4-targeted nanoparticles for induction and maintenance of regulatory T cells, Biomaterials 59 (2015) 172-81.
[19] L. Zhang, L. Wang, K.A. Shahzad, T. Xu, X. Wan, W. Pei, C. Shen, Paracrine release of IL-2 and anti-CTLA-4 enhances the ability of artificial polymer antigen-presenting cells to expand antigen-specific T cells and inhibit tumor growth in a mouse model, Cancer Immunol Immunother 66(9) (2017) 1229-1241.
[20] E.R. Steenblock, T. Fadel, M. Labowsky, J.S. Pober, T.M. Fahmy, An artificial antigen-presenting cell with paracrine delivery of IL-2 impacts the magnitude and direction of the T cell response, The Journal of Biological Chemistry 286(40) (2011) 34883-92.
[21] K.R. Rhodes, J.J. Green, Nanoscale artificial antigen presenting cells for cancer immunotherapy, Mol Immunol 98 (2018) 13-18.
[22] J.V. Kim, J.B. Latouche, I. Riviere, M. Sadelain, The ABCs of artificial antigen presentation, Nat Biotechnol 22(4) (2004) 403-10.
[23] J.C. Sunshine, K. Perica, J.P. Schneck, J.J. Green, Particle shape dependence of CD8+ T cell activation by artificial antigen presenting cells, Biomaterials 35(1) (2014) 269-277.
[24] S.R. Little, D.M. Lynn, Q. Ge, D.G. Anderson, S.V. Puram, J. Chen, H.N. Eisen, R. Langer, Poly-beta amino ester-containing microparticles enhance the activity of nonviral genetic vaccines, Proc Natl Acad Sci U S A 101(26) (2004) 9534-9.
[25] J.A. Champion, S. Mitragotri, Role of target geometry in phagocytosis, Proc Natl Acad Sci U S A 103(13) (2006) 4930-4.
[26] A.N. McMurchy, M.K. Levings, Suppression assays with human T regulatory cells: a technical guide, Eur J Immunol 42(1) (2012) 27-34.
[27] B. Allard, M.S. Longhi, S.C. Robson, J. Stagg, The ectonucleotidases CD39 and CD73: Novel checkpoint inhibitor targets, Immunol Rev 276(1) (2017) 121-144.
[28] L. Antonioli, P. Pacher, E.S. Vizi, G. Hasko, CD39 and CD73 in immunity and inflammation, Trends Mol Med 19(6) (2013) 355-67.
[29] S. Deaglio, K.M. Dwyer, W. Gao, D. Friedman, A. Usheva, A. Erat, J.F. Chen, K. Enjyoji, J. Linden, M. Oukka, V.K. Kuchroo, T.B. Strom, S.C. Robson, Adenosine generation catalyzed by CD39 and CD73 expressed on regulatory T cells mediates immune suppression, J Exp Med 204(6) (2007) 1257-65.
[30] S. Floess, J. Freyer, C. Siewert, U. Baron, S. Olek, J. Polansky, K. Schlawe, H.D. Chang, T. Bopp, E. Schmitt, S. Klein-Hessling, E. Serfling, A. Hamann, J. Huehn, Epigenetic control of the foxp3 locus in regulatory T cells, PLoS Biol 5(2) (2007) e38.
[31] Q. Chen, Y.C. Kim, A. Laurence, G.A. Punkosdy, E.M. Shevach, IL-2 controls the stability of Foxp3 expression in TGF-beta-induced Foxp3+ T cells in vivo, J Immunol 186(11) (2011) 6329-37.
[32] A. Schmidt, M. Eriksson, M.M. Shang, H. Weyd, J. Tegner, Comparative Analysis of Protocols to Induce Human CD4+Foxp3+ Regulatory T Cells by Combinations of IL-2, TGF-beta, Retinoic Acid, Rapamycin and Butyrate, PLoS One 11(2) (2016) e0148474.

[33] J. Matic, J. Deeg, A. Scheffold, I. Goldstein, J.P. Spatz, Fine tuning and efficient T cell activation with stimulatory aCD3 nanoarrays, Nano Lett 13(11) (2013) 5090-7.
[34] A.S. Cheung, D.K.Y. Zhang, S.T. Koshy, D.J. Mooney, Scaffolds that mimic antigen-presenting cells enable ex vivo expansion of primary T cells, Nat Biotechnol 36(2) (2018) 160-169.
[35] J.K. Polansky, K. Kretschmer, J. Freyer, S. Floess, A. Garbe, U. Baron, S. Olek, A. Hamann, H. von Boehmer, J. Huehn, DNA methylation controls Foxp3 gene expression, Eur J Immunol 38(6) (2008) 1654-63.
[36] U. Baron, S. Floess, G. Wieczorek, K. Baumann, A. Grutzkau, J. Dong, A. Thiel, T.J. Boeld, P. Hoffmann, M. Edinger, I. Turbachova, A. Hamann, S. Olek, J. Huehn, DNA demethylation in the human FOXP3 locus discriminates regulatory T cells from activated FOXP3(+) conventional T cells, Eur J Immunol 37(9) (2007) 2378-89.
[37] J. Huehn, J.K. Polansky, A. Hamann, Epigenetic control of FOXP3 expression: the key to a stable regulatory T-cell lineage?, Nat Rev Immunol 9(2) (2009) 83-9.
[38] A.K. Kosmides, R.A. Meyer, J.W. Hickey, K. Aje, K.N. Cheung, J.J. Green, J.P. Schneck, Biomimetic biodegradable artificial antigen presenting cells synergize with PD-1 blockade to treat melanoma, Biomaterials 118 (2017) 16-26.

FIGURES

Figure 1

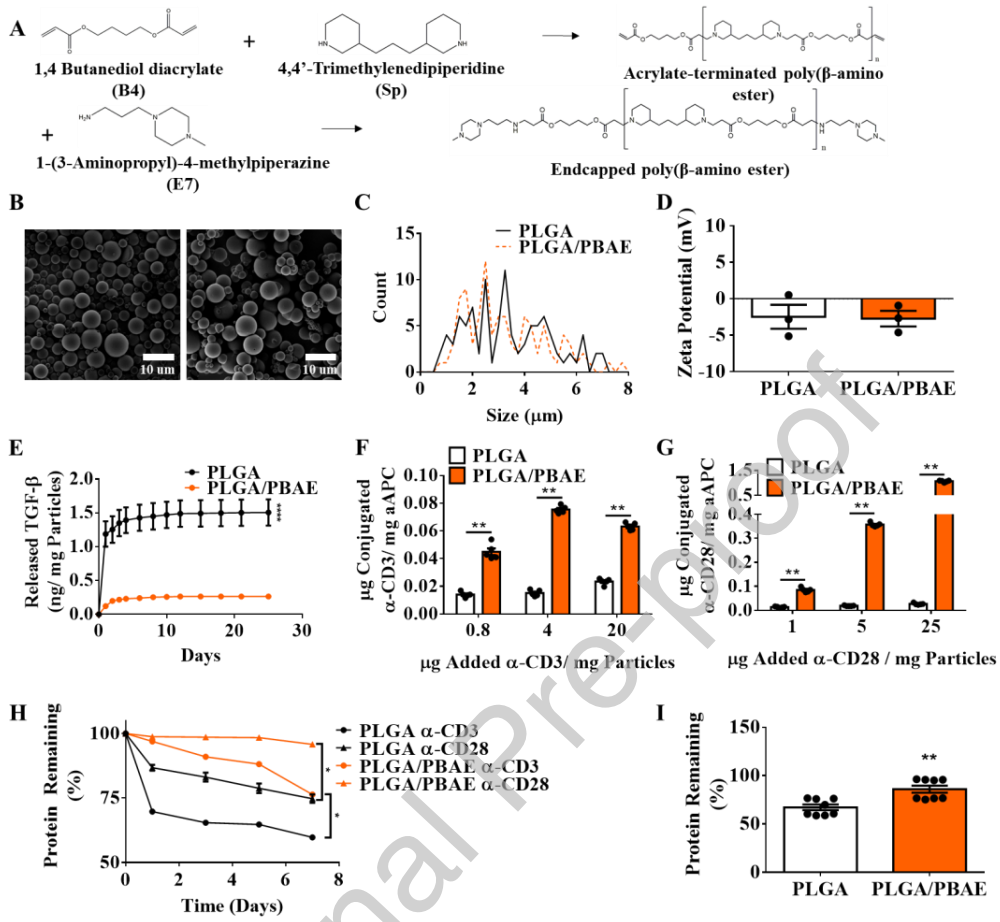

Figure 1: aAPC synthesis and characterization. **A)** PBAE was synthesized through two sequential Michael Addition reactions. First, a diacrylate-terminated base monomer was reacted in excess with a hydrophobic diamine-terminated side chain monomer to generate a diacrylate-terminated PBAE. The base PBAE polymer was then endcapped with a small amine-terminated molecule. **B)** SEM images of PLGA (left) and PLGA/PBAE (right) microparticles reveal similar size and spherical morphology. **C)** PLGA and PLGA/PBAE microparticles have similar size distributions. **D)** PLGA and PLGA/PBAE microparticles have slightly negative zeta potentials. **E)** TGF- β release from PLGA and PLGA/PBAE particles. **F-G)** Protein conjugation to PLGA and PLGA/PBAE particles. PLGA/PBAE aAPCs conjugate significantly more **F)** α-CD3 and **G)** α-CD28 to their surface compared to PLGA aAPCs across a range of protein doses added during conjugation. **H)** Surface protein stability. PLGA/PBAE aAPCs retain significantly more surface-bound α-CD3 and α-CD28 over a 7-day period compared to PLGA aAPCs. Error bars may be smaller than symbols. **I)** Average percent of surface protein remaining on aAPCs after 7 days. PLGA/PBAE retain 86 % stable protein presentation on their surface after 7 days at 37°C while PLGA aAPCs retain 67%. Error bars are the SEM of 3-8 technical replicates and may be smaller than symbols. (**=p<0.01, ****=p<0.0001).

Figure 2

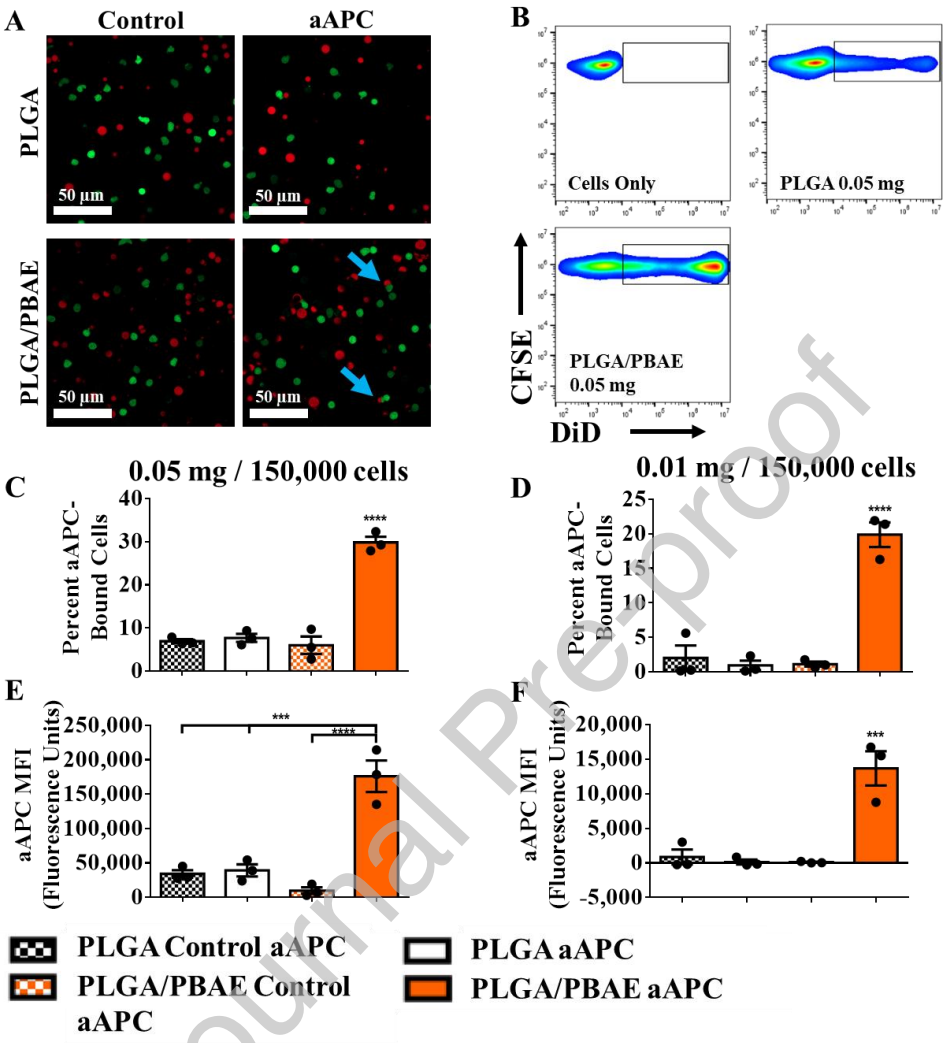

Figure 2: PLGA/PBAE aAPCs interact more with naïve CD4+ T cells compared to PLGA aAPCs. **A)** Confocal images of fluorescent PLGA and PLGA/PBAE aAPC binding to fluorescently labelled naïve CD4+ T cells. Blue arrows indicate binding events. **B)** Representative plots of flow cytometric analysis of aAPC/ T cell binding. **C)** Significantly more naïve CD4+ T cells bind to PLGA/PBAE aAPCs compared to PLGA aAPCs at a 0.05 mg **D)** 0.01 mg doses. **E)** Mean fluorescence intensity of PLGA/PBAE aAPC/ cell complexes is significantly higher than PLGA aAPC/ cell complexes, indicating that cells contain higher numbers of bound aAPCs at a 0.05 mg dose and **F)** 0.01 mg dose. Error bars are the SEM of three technical replicates. (***=$p < 0.001$, ****=$p < 0.0001$).

Figure 3

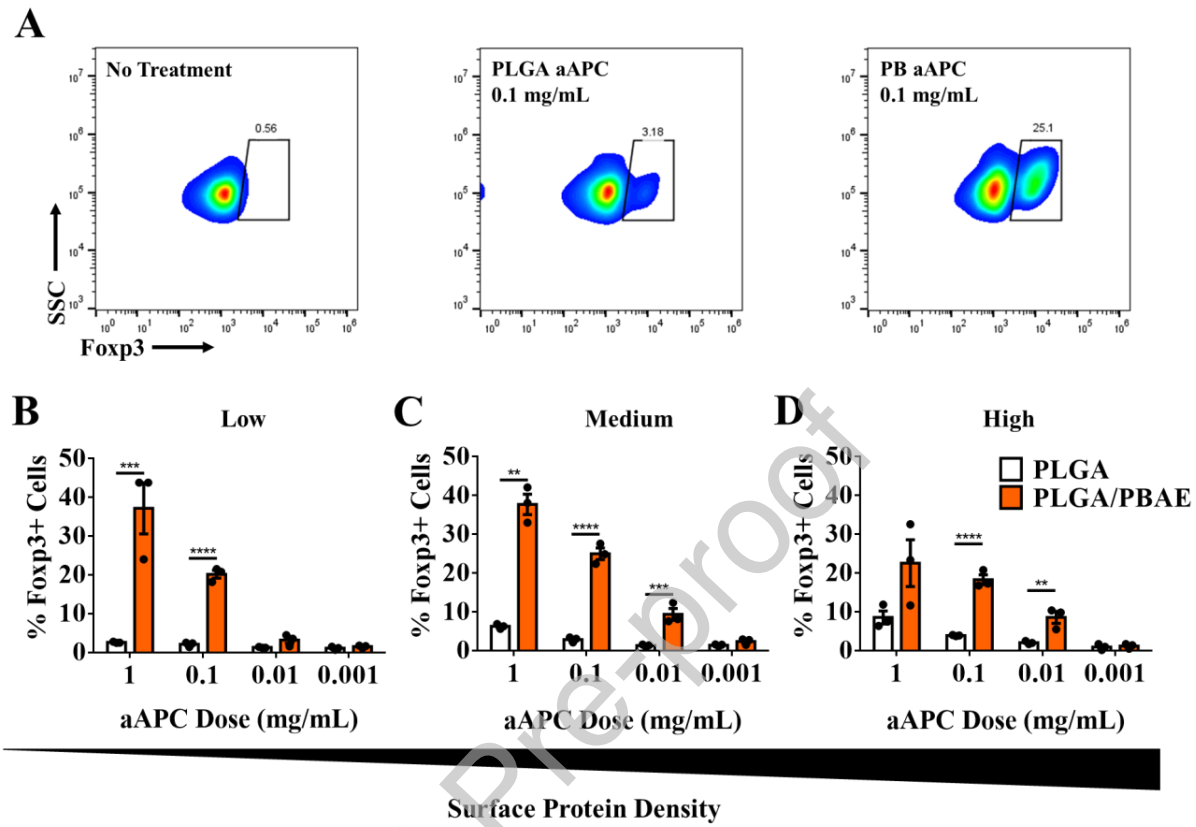

Figure 3: PLGA/PBAE aAPCs induce significantly more iTregs compared to PLGA aAPCs. **A)** Representative flow plots. PLGA and PLGA/PBAE aAPCs conjugated with **B)** 1/5x **C)** 1x and D) 5x signal protein densities were incubated with naïve CD4+ T cells in the presence of TGF-β and IL-2 for five days, and then stained for Foxp3 (FJK-16s) – APC. Enhanced induction efficacy of PLGA/PBAE aAPCs was seen over a range of aAPC doses. Error bars are the SEM of three technical replicates. (**=$p < 0.01$, ***=$p < 0.001$, ****=$p < 0.0001$).

Figure 4

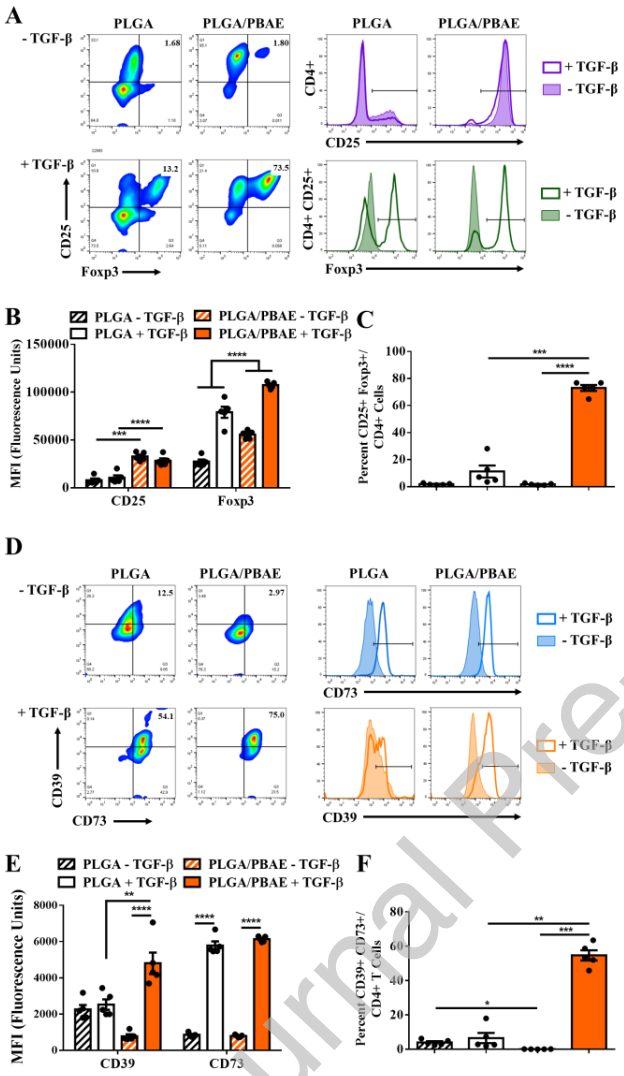

Figure 4. TGF-β is required for PLGA and PLGA/PBAE aAPC-mediated Treg induction. **A)** PLGA and PLGA/PBAE aAPCs were incubated with naïve T cells for 5 days with IL-2 ± TGF-β, then stained for CD4 (RM4-5) – AF 488, CD25 (PC61) - PE, Foxp3 (FJK-16s) – Pacific Blue, CD39 (Duha59) - APC, and CD73 (TY/11.8) – APC/Fire 750. PLGA/PBAE aAPC mediate enhanced iTreg induction compared to PLGA aAPCs as evidenced by increased Foxp3 expression. **B)** PLGA/PBAE aAPC-treated CD4+ T cells show increased levels of CD25 and Foxp3 compared to PLGA aAPC-treated cells. **C)** PLGA/PBAE aAPC treatment increases the percentage of CD25+ Foxp3+ iTregs compared to PLGA in the presence of TGF- β. **E)** CD25+ Foxp3+ iTregs induced by PLGA/PBAE aAPCs and TGF-β show increased levels of CD39 and CD73 expression compared to CD25+ cells induced in the absence of TGF- β. **F)** PLGA/PBAE aAPC treated CD4+ T cells co-express CD39 and CD73 when cultured in the presence of TGF-β. Error bars are the SEM of five technical replicates. (*=p < 0.05, **=p < 0.01, ***=p < 0.001, ****=p < 0.0001).

Figure 5

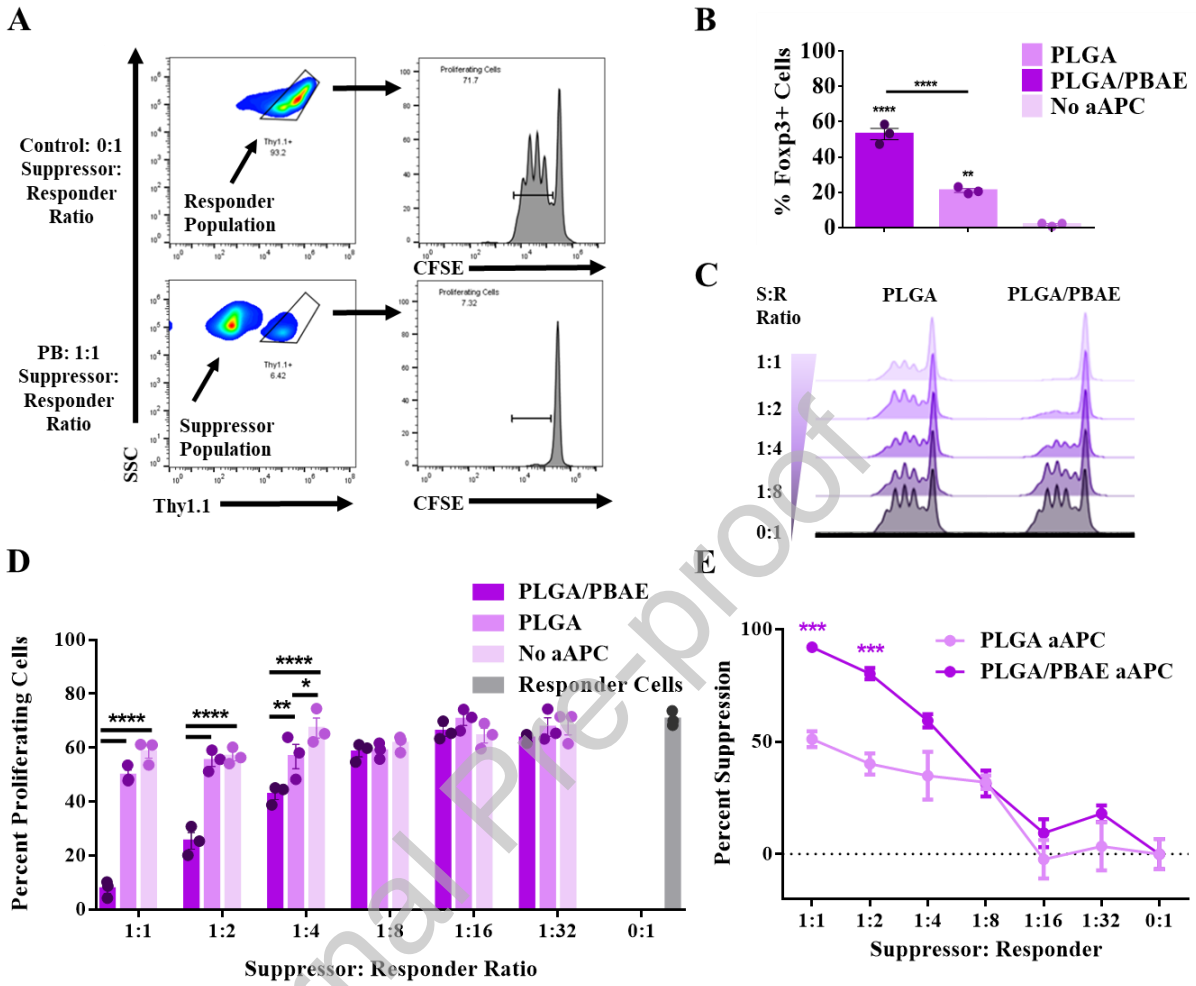

Figure 5: Cell populations induced by PLGA/PBAE aAPCs more effectively suppress proliferation of naïve CD4+ T cells compared to those induced by PLGA aAPCs. A) Gating strategy for *in vitro* suppression assay. CFSE-labelled responder cells were stained for Thy1.1 (OX-7) – APC. CFSE dilution peaks were used to ascertain the fractions of proliferating and nonproliferating Thy1.1+ responder cells. **B)** Foxp3 expression in suppressor populations after a five-day induction period with PLGA aAPCs, PLGA/PBAE aAPCs, or cytokines TGF-β and IL-2 only. **C)** CFSE dilution peaks of responder population at various suppressor/responder ratios. Less proliferation is seen in responder populations incubated with PLGA/PBAE aAPC-induced suppressor populations. **D-E)** Suppressor populations induced with PLGA/PBAE aAPCs significantly suppress responder proliferation compared to those induced by PLGA aAPCs or a cytokine control at multiple suppressor-to-responder ratios based on the percentage of **D)** proliferating CFSE+ responder cells or **E)** percent suppression calculated using the division index. Error bars represent the SEM of three technical replicates and may be smaller than symbols. (*=$p < 0.05$, **=$p < 0.01$, ***=$p < 0.001$, ****=$p < 0.0001$).

Figure 6

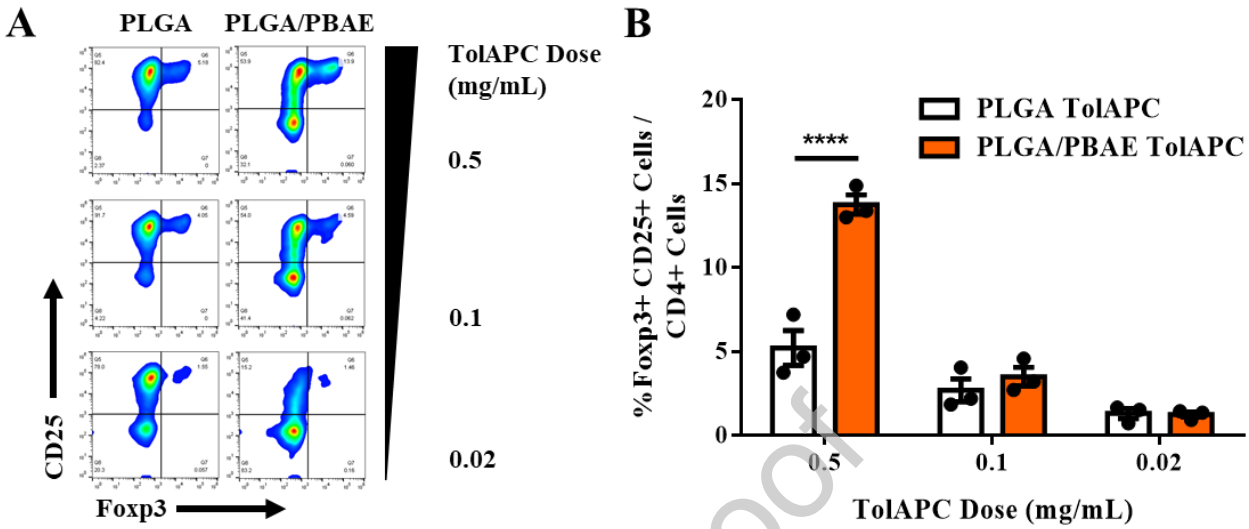

Figure 6. PLGA/PBAE loaded with TGF- β generate iTregs. Naïve CD4+ T cells were incubated with TolAPCs and IL-2 for 4 days, then stained for CD4, CD25, and Foxp3. A) Flow cytometry plots showing CD25 and Foxp3 fluorescence within the CD4+ T cell population. B) PLGA/PBAE TolAPC induce Foxp3+ Tregs in a dose-dependent manner and are superior to PLGA TolAPC at a dose of 0.5 mg/mL. Error bars represent the SEM of three technical replicates (****=$p < 0.0001$).

Figure 7

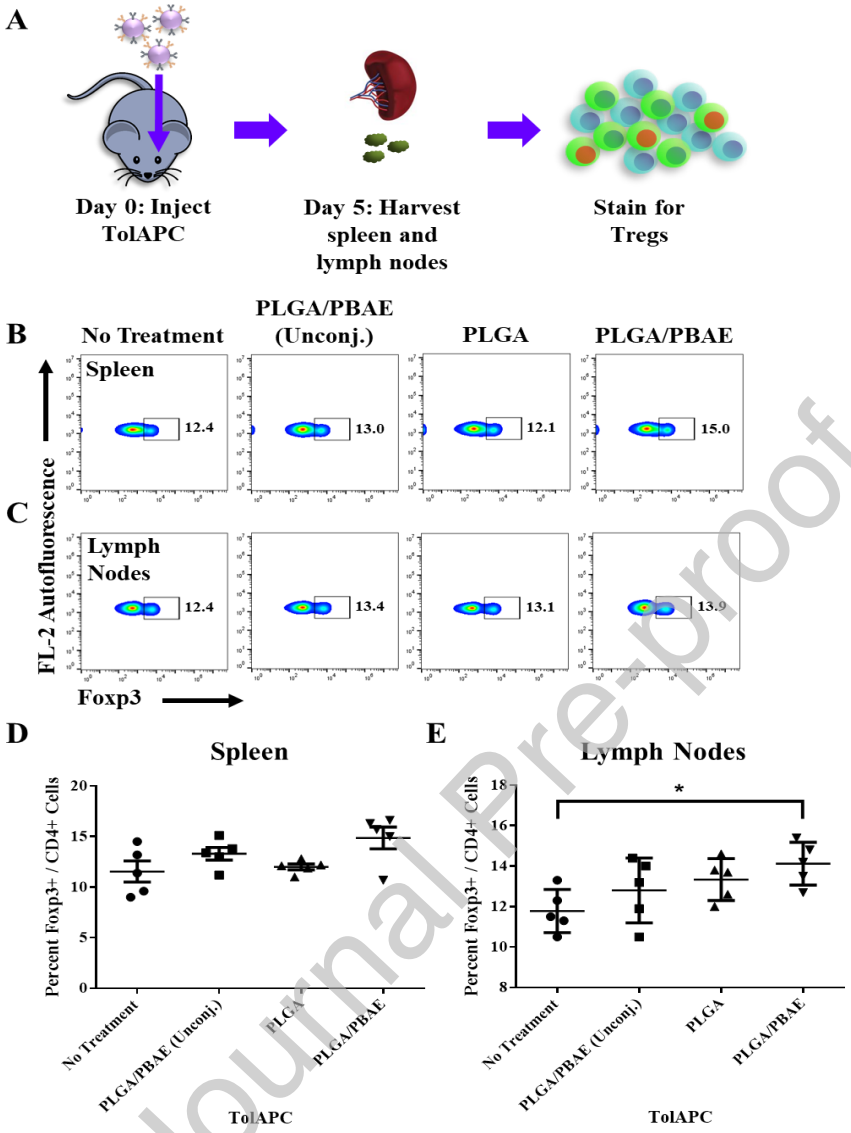

Figure 7: PLGA/PBAE TolAPCs more effectively induce Tregs *in vivo*. A) TolAPCs were injected retroorbitally into C57BL/6J mice. After 5 days, the spleens and lymph nodes were harvested and stained for CD4 and Foxp3 expression. Representative flow plots showing CD4+ cells from **B)** spleens and **C)** lymph nodes of mice. **D)** Spleens and **E)** lymph nodes of C57BL/6J mice injected with PLGA/PBAE TolAPCs contained more Foxp3+ cells than those injected with PLGA TolAPCs, and significantly increase the percentage of Foxp3+ cells compared to untreated mice in the lymph nodes. Error bars represent the SEM with n = 5 animals per condition. **D)** is significant based on an ANOVA, $p < 0.5$. (*=$p < 0.05$, only conditions marked with (*) are significant and all other comparisons were performed and found to be not significant.)